Resonant ultrasound spectroscopy: theory and application

Brian Zadler, John A. Scales and Jérôme H.L. Le Rousseau, Center for Wave Phenomena and Physical Acoustics Laboratory, Colorado School of Mines, Martin L. Smith, New England Research*

Summary

Resonant Ultrasound Spectroscopy (RUS) uses normal modes of elastic bodies to infer material properties such as elastic moduli and Q. In principle, the complete elastic tensor can be inferred from a single measurement. For centimeter-sized samples RUS fills an experimental gap between low-frequency stress-strain methods (quasi-static up to a few KHz) and ultrasonic time-delay methods (hundreds of KHz to GHz). We find RUS to be consistent with ultrasonic time delay measurements for samples with both high (isotropic) and low (orthorhombic) symmetries. We have applied the technique to macor, a material with properties simialar to aluminum, and have shown that it was isotropic. For Elberton granite, the symmetry had to be lowered to orthorhombic to achieve a significant fit. The 10% inferred anisotropy of the sample was confirmed via laser ultrasonic measurements. With such accurate results during bench-top measurements, we are now applying the same methods to multi-component systems under confining pressure and partial saturation.

Introduction

Upon excitation, elastic bodies isolated in free space oscillate at discrete frequencies. These normal modes can be observed and measured. The geometry and size of the system strongly influence the range of frequencies at which such normal modes occur. For a 10 centimeter pieced of sandstone, the fundamental mode has a frequency of about 10 kHz. The elastic moduli also influence the resonance frequencies: the stiffer the sample, the higher frequencies. The idea behind resonant ultrasound spectroscopy (RUS) is to use these dependencies to infer elastic properties or shape parameters of samples from a suite of measured resonance frequencies.

Our algorithms allow us to apply RUS to a variety of regular geometries. We calculate the normal modes of an elastic body and cast them into a generalized eigenvalue problem via a Rayleigh-Ritz method. We solve this eigenvalue problem using standard numerical tools. The inverse problem is then formulated for the components of the elastic tensor as a least-squares fitting of the predicted to measured normal-mode frequencies. We skip the discussion of the forward modeling and inversion theory, most of which is outlined in detail such books as *Resonant Ultrasound Spectroscopy* (Migliori & Sarrao, 1997).

In the following sections we discuss the theory of measuring the resonance spectrum of a sample and extracting the eigenfrequencies. We then follow up with a quick explanation on extracting meaningful results from our measurements. Finally, we show application of the RUS method to rock samples, both isotropic and anisotropic. Software implementing all aspects of the calculation (spectra fitting and least squares inversion) is freely available upon request from authors.

height	1.22	inches
radius	0.25	inches
density	2.5	gm/cm^3
V_P	3.000	km/sec
V_S	1.400	km/sec

Table 1: Properties of a *generic soft rock* similar to shale.

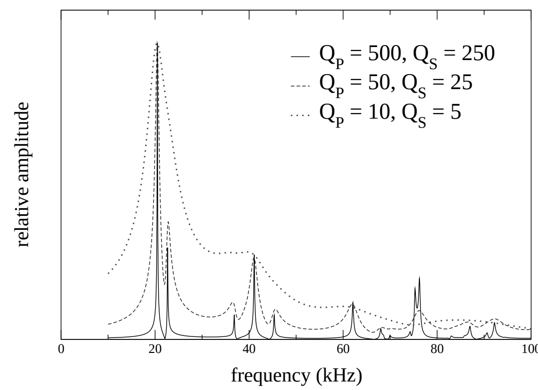

Fig. 1: The theoretical resonance response of a generic soft rock sample defined in Table 1 for high, moderate, and low values of compressional and shear Q.

Excitation and Observation

In typical RUS measurements, we try to measure all of the resonances below some upper limit. Having a complete set of resonances assures us that we have extracted all of the available information and significantly simplifies the inverse calculation.

For a pedagogical example, imagine a material with properties that are similar to a shale and refer to the material as *generic soft rock.* Its properties are defined in Table 1.

Figure 1 shows the theoretical resonance response of a cylindrical sample of the *generic soft rock* using the edge-contacting pinducer arrangement shown in Figure 2. The three cases represent, by geologic standards, very high, moderate, and low compressional and shear Q regimes. It is clear that we cannot depend upon observing a complete mode catalog within a particular frequency interval in the presence of even moderate attenuation.

Figure 2 shows the computed response for the generic soft

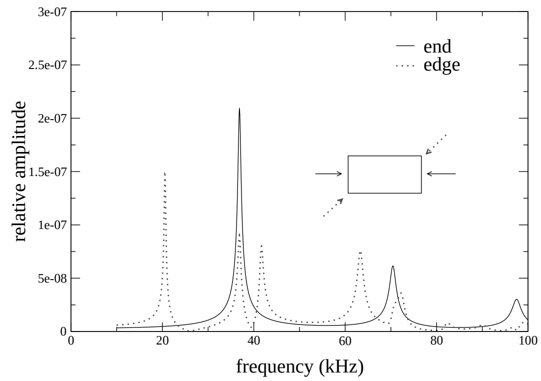

Fig. 2: The theoretical resonance response of our generic soft rock sample for the edge and end mounted transducer configurations.

rock sample for two transducer arrangements for moderate values of Q. The important point to note is that there are modes that appear prominently in the *edge* spectrum that are missing from the *end* spectrum.

These results tell us that developing the ability to get V_P and V_S in a single experiment will probably involve a more sophisticated edge-contacting transducer or an alternate transducer arrangement that favors particular modes of excitation. As the measured system moves toward *in situ* conditions, it may become necessary to constrain mode calculation and inversion to a particular subset of frequencies. We do not yet have a global solution to the resonance experiment design problem.

Data acquisition

A function generator sends a 10 Volt (peak-peak) swept sine wave to the source transducer. This signal is detected synchronously with a DSP lock-in amplifier, which digitizes the input and reference signal with 18 bit precision, directly measuring the in-phase and quadrature components. Amplitude and phase are calculated from these.

In the first measurements, to limit loss of energy and control the humidity in the bench top measurements we place the sample in a vacuum chamber held at -65 KPa at room temperature, 23 C. In our theoretical derivations we did not implement boundary and radiation conditions. With the use of the vacuum chamber in the experiments we can stick to those assumptions. The vacuum chamber also yields a quieter environment for the experiment. For porous media even a single mono-layer of water adsorbed onto the pore space of the sample can have a dramatic influence on the moduli.

Identification of normal mode frequencies

The eigenfrequency of a mode is not exactly at the maximum of the corresponding peak in the spectrum. Any one mode is assumed to have Lorentzian shape, and multiple overlapping modes are considered to be a superposition of Lorentzians. Examples of this shape can be seen in Figure 2. The model we used to fit the amplitudes of one or multiple modes is due to Briet and Wigner (Breit & Wigner, 1936):

$$A(f) = B_0 + B_1(f - f_0) + \sum_{n}^{N} \frac{C_n + D_n(f - f_0)}{(f - f_n)^2 + \frac{1}{4}\Gamma_n^2} \qquad (1)$$

where the displacement amplitude A is a function of frequency. The parameters B_0 and B_1 describe a constant and linear background, respectively. The shape of each mode is then defined via 4 parameters: amplitude C_n, skewness D_n, eigenfrequency f_n and full width at half maximum Γ_n. Therefore, a simultaneous fit of n resonance peaks will require $4 \times n + 2$ parameters.

A non-linear least squares fit of the data is performed. Since the fit is sensitive to the initial parameters, they need to be chosen carefully and accurately. It would be preferable to fit the modes one peak at a time, but this is not always possible due to degenerate and overlapping modes.

In high Q materials the peaks are relatively narrow and splitting of degenerate peaks is easier to detect. Figure 1 shows how difficult it can be to identify a set of consecutive modes for low Q specimens. This leads us to the conclusion that modeling the effects of the transducers to predict the amplitude response may be necessary.

The other source of difficulty in eigenfrequency identification comes from the coupling of the sample to the apparatus. Slight differences in the positioning of the sample between the pinducers contribute to this uncertainty. Fortunately, this error can be estimated by completely mounting and remounting the same sample. Although this is feasible for bench-top measurements, it would likely be too time consuming or impossible for semi-permanently mounted transducers in *in situ* measurements.

Experimental results

Missing a normal mode during measurement can be fatal to the inversion if a shift between the measured and computed frequencies appears. The optimization may converge to a local extremum. To avoid this problem, we use sets of peaks we are confident in to perform the inversion. We can also use the weight (inverse data standard deviation) w_i in the objective function

$$F = \sum_i w_i (f_i^{(p)} - f_i^{(m)})^2 \ , \qquad (2)$$

where $f^{(p)}$ are the computed frequencies and $f^{(m)}$ are the measured ones. Lower weight would be associated with measured frequencies in which we have low confidence; although we will directly estimate the variance in the measured eigenfrequencies later.

The first iterations of the inversion are done with low order polynomials (N=5-7). These approximations can rapidly predict the first few mode frequencies accurately but fail to accurately predict higher modes. Higher order polynomials considerably increase the computation time but yield a better resolution using information of higher normal modes. Along with the different iterations, new information becomes new *a priori* information for the next iterations. We usually start with an isotropic model. If a proper fit cannot be achieved we lower the symmetry of the model used: cubic, then hexagonal, etc.

The following results show that we can achieve a model that fits our data. Uncertainties can arise from a number of sources. What we need to know is if a model fits the data in a statistically significant way. We implement this in two ways. First, in our non-linear conjugate gradient method we assume to have found an answer when the gradient is lower than a certain threshold. Deciding on this threshold depends on the confidence we have in our data and what noise level we have. Second, we use a χ^2 test to know if a proper fit to the elastic moduli has been achieved.

In using the χ^2 test, it is necessary to know the uncertainty σ_i in frequency for each observed eigenfrequency f_i^{obs}. To obtain these values, we assume that only physical mounting of the sample contributes to the uncertainty. By completely mounting and unmounting a sample N times, we get N realizations of each spectrum. Then for the ith mode we calculate a mean eigenfrequency f_i and standard deviation σ_i.

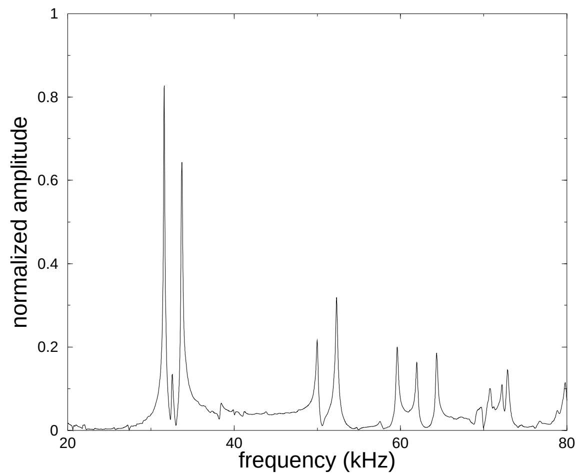

Fig. 3: Spectrum of a cylindrical granite core (2.27 cm × 2.27 cm × 7.15 cm). A sweep from 20 to 100 kHz with a 5Hz step was applied.

Granite cylinder

We have applied our RUS techniques to a variety of samples, including isotropic, anisotropic, synthetic materials and rock. Here we show the case of a 75 mm by 25 mm cylindrical core of Elberton granite. An example of a measured spectrum can be seen in Figure 3. In order to get our uncertainty estimates for calculating a χ^2 value of our fit model, the granite sample was completely mounted and unmounted 14 times. The mean eigenfrequencies and their corresponding uncertainties are shown in Table 2. Frequency uncertainty ranged from 22 Hz to 801 Hz with a mean uncertainty of 258 Hz. Although the amplitudes seemed to vary greatly for specific modes, the measured Q values of the modes were fairly stable ranging from approximately 100 to 200, with an average uncertainty of 41.

A first attempt to match the first six normal modes with an isotropic model was unsuccessful. Larger frequencies could not be fitted at all. We then tried anisotropic models with lower and lower symmetries. Finally with the use of an orthorhombic model, we can achieve a fit of 25 consecutively measured resonances with a χ^2 of about 38. The comparison between predicted and measured frequencies can be found in Table 2. The inverted model is $c_{11} = 67.87 \pm 1.14$GPA, $c_{22} = 81.94 \pm 0.70$GPA, $c_{33} = 81.83 \pm 0.69$GPA, $c_{23} = 27.15 \pm 1.10$GPA, $c_{13} = 28.95 \pm 0.86$GPA, $c_{12} = 39.76 \pm 0.14$GPA, $c_{44} = 23.72 \pm 0.02$GPA, $c_{55} = 29.16 \pm 0.01$GPA and $c_{66} = 28.67 \pm 0.01$GPA. In the anisotropic symmetry plane this yields qP wave speeds of

t $f^{(obs)}$ (MHz)	$f^{(pre)}$ (MHz)	$\sigma^{(obs)}$ (Hz)	freq. #
0.031490	0.031490	50	4
0.032380	0.031680	58	5
0.033620	0.032540	29	6
0.049670	0.050080	31	8
0.052280	0.052230	43	9
0.059500	0.059400	22	10
0.061970	0.061960	27	11
0.064380	0.065220	39	12
0.069760	0.070050	75	13
0.071860	0.071800	801	14
0.072330	0.072310	327	15
0.075700	0.075750	376	16
0.076020	0.076070	411	17
0.078200	0.078300	396	18
0.079200	0.078640	401	19
0.079200	0.079256	406	20
0.081080	0.080978	789	21
0.084800	0.084833	393	22
0.085600	0.085088	575	23
0.086800	0.087480	394	24
0.087500	0.087512	569	25

Table 2: Comparison between the observed $f^{(obs)}$ and predicted $f^{(pre)}$ normal frequencies with uncertainties for an Elberton granite core.

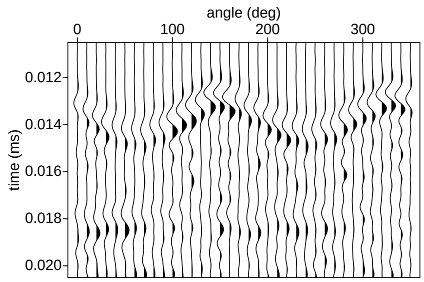

Fig. 4: Laser ultrasonic measurement of waves traveling straight across a 5.5 cm diameter granite core. A pulsed IR laser in the thermoelastic regime is used to excite elastic waves which are measured with a laser Doppler vibrometer. The sample is rotated 10 degrees between measurements. For more details see (Malcolm & Scales, 2002).

5003±21 m/s and 4556±38 m/s in the vertical and horizontal directions respectively. This nearly 10% P-wave anisotropy is consistent with ultrasonic measurements as shown in Figure 4.

In the same symmetry plane the S wave speeds are 2986±5 m/s for the vertical polarization, 2694±10 m/s and 2961±5 m/s for the horizontal polarization in the vertical and horizontal directions respectively. Also note the difference in values for the other decoupled coefficients, c_{12} and c_{23}, c_{11} and c_{22}. Here our χ^2 test was used as a tool to decide the symmetry of the sample. Granite is known to be anisotropic. The way granite is extracted and cut in quarries takes advantage of that anisotropy. This ensured, fortunately, that for such a sample we have the anisotropic symmetry axis coinciding with the geometrical symmetry axis of the sample. This makes our assumptions valid in this case. Otherwise, we would have to invert for the crystallographic axis as well.

Conclusion

RUS methods have been used extensively in the materials science community to evaluate high-Q crystals of small sizes. The method then yields an efficient way to invert for elastic properties. In this paper we show that this method is quite robust and that it may be applied to larger object and also objects that have small-scale heterogeneities such as rocks. We have, so far, only studied clean, relatively homogeneous rock samples, using normal modes whose wavelengths are large compared to the granularity of the sample. For samples with large-scale heterogeneity, it will presumably be necessary to perform a preliminary analysis (e.g., tomography) to characterize the sample. Nevertheless, RUS can be applied to rock samples. RUS fills an experimental gap between low frequency stress-strain methods and high frequency ultrasonic delay times. RUS allows us to infer the complete elastic tensor in a single measurement.

Current measurements are under way to apply RUS to

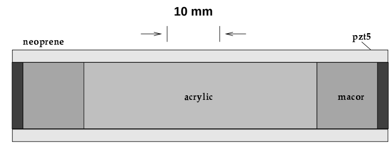

Fig. 5: Scale drawing of the jacketed acrylic sample.

real and synthetic rocks under confining pressure while partially saturated. This involves a setup similar to Figure 5 in which the jacket material and the transducers are bonded together.

Acknowledgment

We thank Lydia H. Deng for her help with the COOOL library, Mike Batzle for his help in the sample preparation and Gary R. Olhoeft for valuable comments. This work was partially supported by the National Science Foundation (EAR-0111804), the members of the consortium project on Seismic Imaging of Complex Structures at the Center for Wave Phenomena, CSM and the members of the consortium project on Fluids, Center for Rock Abuse, CSM.

References

Breit, G., and Wigner, E., 1936, Capture of slow neutrons: Physical Review, **49**, 519.

Malcolm, A., and Scales, J., 2002, Seeing heterogeneities in rocks: preliminary results from a noncontacting ultrasonic experiment: preprint.

Migliori, A., and Sarrao, J. L., 1997, Resonant ultrasound spectroscopy: applications to physics, materials measurements, and non-destructive evaluation: , John Wiley & Sons, INC., New York.